

## Sea ice thickness in the southwestern Sea of Okhotsk revealed by a moored ice-profiling sonar

Yasushi Fukamachi,<sup>1</sup> Genta Mizuta,<sup>2</sup> Kay I. Ohshima,<sup>1</sup> Takenobu Toyota,<sup>1</sup> Noriaki Kimura,<sup>1</sup> and Masaaki Wakatsuchi<sup>1</sup>

Received 29 September 2005; revised 27 January 2006; accepted 23 May 2006; published 14 September 2006.

[1] Using a moored ice-profiling sonar along with a moored acoustic Doppler current profiler, a total spatial section of draft across 3334 km of sea ice was obtained in the southwestern Sea of Okhotsk near Hokkaido in the winters of 1999–2001. Using this draft data set, the average draft and keel statistics are discussed in this sea for the first time. The mean draft was 0.60 m, which corresponds to the thickness of 0.71 m, over the three winters with the range of 0.49–0.72 m for each winter. The classification of level and deformed ice reveals a small range of the monthly mean level ice draft (0.18–0.27 m) and the dominance of the deformed ice in terms of volume (80%). The mean draft varied with the areal ratio of the deformed ice fairly well. These results suggest that dynamic processes such as ridging and rafting are important for the evolution of draft in the region of observation. The observed draft probability density distribution and keel statistics show that the thick ice ratio and keel frequency are lower than the similar data in polar regions and closer to those observed in Davis Strait west of Greenland. Along with the ice concentration and speed derived from the satellite data the southward ice transport to the southwestern Sea of Okhotsk is estimated on the basis of the observed sea ice thickness. The estimated ice transport ranged from 15 to 70 km<sup>3</sup> in each winter. The heat and freshwater transport associated with the ice transport ranged from  $-3.9 \times 10^{17}$  to  $-1.8 \times 10^{18}$  J and from 12 to 57 km<sup>3</sup>, respectively.

**Citation:** Fukamachi, Y., G. Mizuta, K. I. Ohshima, T. Toyota, N. Kimura, and M. Wakatsuchi (2006), Sea ice thickness in the southwestern Sea of Okhotsk revealed by a moored ice-profiling sonar, *J. Geophys. Res.*, *111*, C09018, doi:10.1029/2005JC003327.

### 1. Introduction

[2] The Sea of Okhotsk (Figure 1) is the southernmost sea ice area in the Northern Hemisphere except areas of coastal freezing. Because of this location, climate change can significantly alter the amount of sea ice in this sea. Sea ice extent is highly variable from year to year [e.g., Parkinson, 1990] (also see Figure 2). However, annual variability has been discussed on the basis of ice area not on ice volume because of the lack of in situ observations and remote sensing capability for ice thickness. In fact, systematic ice thickness observations are fairly limited in the Sea of Okhotsk. In the southwestern part of the sea, Toyota and Wakatsuchi [2001] and Toyota *et al.* [2004] carried out ship-based monitoring to measure thickness of ice floes turned into side-up positions with a downward looking video camera in 1996–2004 (Figure 3). Although this monitoring covered most of the area off Hokkaido, the temporal coverage was limited and the method is not

capable of measuring thick floes because they are not likely to turn into side-up positions.

[3] Recently, mooring observations of the upward looking sonar or ice-profiling sonar (IPS) have been carried out in various areas to reveal the variability of ice draft [Melling and Riedel, 1995, 1996; Strass and Fahrbach, 1998; Vinje *et al.*, 1998; Worby *et al.*, 2001; Harms *et al.*, 2001; Drucker *et al.*, 2003]. This method is capable of measuring ice draft of any thick floes. In the area off the northern coast of Sakhalin, Birch *et al.* [2000] and Marko [2003] carried out moored IPS observations during winters of 1996–1997 and 1997–1998. These were the first IPS observations in the Sea of Okhotsk but a full description of the data and results is not available. Fukamachi *et al.* [2003] carried out the IPS observation near Hokkaido in the southwestern Sea of Okhotsk during the winter of 1999. They showed the average draft during this winter and the dominance of the deformed ice in this region.

[4] In this paper, the results of Fukamachi *et al.* [2003] are extended by combining the similar data obtained in winters of 2000 and 2001 with those in 1999. As a result, various draft and keel statistics, which have been revealed in other high-latitude oceans, are discussed for the first time in the Sea of Okhotsk on the basis of the multiyear, time series data. Furthermore, the factors determining draft are examined. Finally, the southward ice transport, which accompa-

<sup>1</sup>Institute of Low Temperature Science, Hokkaido University, Sapporo, Japan.

<sup>2</sup>Graduate School of Environmental Science, Hokkaido University, Japan.

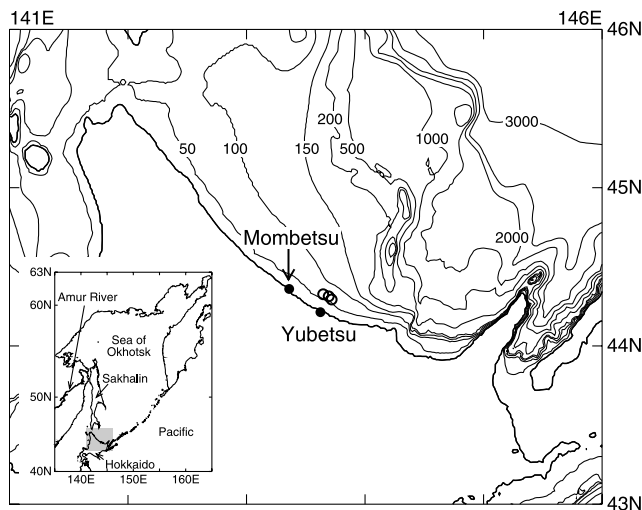


**Figure 1.** A map showing the locations of the moorings (denoted by open circles). Three locations from the northwest to southeast were for 1999, 2000, and 2001, respectively. The atmospheric pressure and surface wind data used in this research were measured in Mombetsu and Yubetsu (denoted by solid circles), respectively. The inset map shows the entire Sea of Okhotsk. The shading denotes the region of the enlarged map. Bathymetry data are extracted from the General Bathymetric Chart of the Oceans.

nies heat and freshwater transport, to the southwestern part is estimated for the first time using the measured ice thickness data.

## 2. General Ice Conditions

[5] Before discussing the data in the present observations, the general ice conditions in the Sea of Okhotsk are briefly summarized here. Sea ice first forms near the northern and northwestern coasts in November, then spreads southward along Sakhalin and eventually reaches Hokkaido typically by mid-January. Maximum ice extent normally occurs in early March. Finally, it retreats from Hokkaido in early April.

[6] Sea ice extent on 5 March, which is around the normal peak period, was quite different in 1999–2001 (Figures 2a–2c). Actually, the maximum extent of  $122$ ,  $134$ , and  $152 \times 10^4 \text{ km}^2$  was observed on 31, 20 and 5 March in 1999, 2000, and 2001, respectively. The maximum extent was more than the average ( $114 \times 10^4 \text{ km}^2$ ) over 1970–2000 during all three winters. (Figure 2d shows the average ice extent over 1988–2004 when the SSM/I data are available.) Especially, the maximum extent in 2001 was the largest after 1979 and 97% of the sea was covered by ice [Japan Meteorological Agency, 2001]. The average sea ice concentration in the coastal area off Hokkaido (within  $\sim 60 \text{ km}$  from the coast) observed by sea ice radars was 36, 52, and 56% during January–March in 1999, 2000, and 2001, respectively [Ishikawa *et al.*, 2001]. Both the arrival and retreat of sea ice to and from the coast of Hokkaido occurred later, around, and earlier than normal in

1999, 2000, and 2001, respectively [Japan Meteorological Agency, 2001].

[7] In 2000 and 2001, the mooring period covered the entire sea ice season around the mooring locations. In 1999, however, sea ice returned to the region around the mooring location in mid-April after the recovery of the moorings.

## 3. Data and Processing

[8] The moorings were deployed at slightly different locations to avoid fishing activities in three years (Figure 1 and Table 1). They were located  $\sim 11 \text{ km}$  off the northeastern coast of Hokkaido, where the water depths are 56–59 m. The moorings contained an IPS (ASL Environmental Sciences IPS4 420 kHz) and an acoustic Doppler current profiler (ADCP) (RD Instruments WH-Sentinel 300 kHz). They were deployed in separate moorings ( $\sim 300 \text{ m}$  apart) to avoid possible acoustic interference. Both of the IPS and ADCP were moored  $\sim 14 \text{ m}$  above

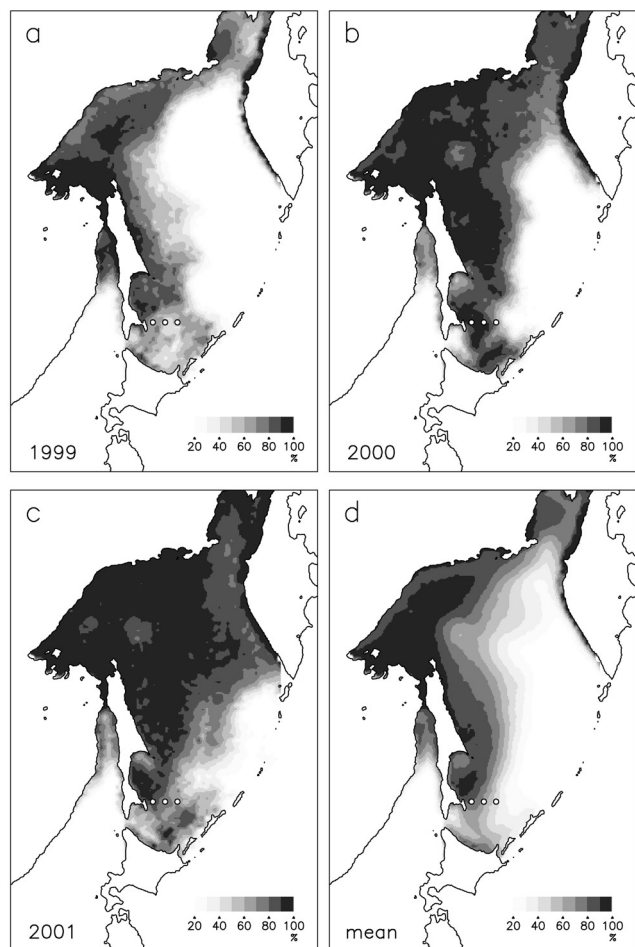


**Figure 2.** Sea ice concentration on 5 March in the Sea of Okhotsk in (a) 1999, (b) 2000, (c) 2001, and (d) the mean in 1988–2004 based on the SSM/I data. Three circles off the southern Sakhalin are SSM/I grids whose data are used for the southward ice transport estimate in section 5.2. Their locations are  $(46^\circ 30.0' \text{N}, 144^\circ 5.6' \text{E})$ ,  $(46^\circ 24.1' \text{N}, 144^\circ 56.9' \text{E})$ , and  $(46^\circ 17.6' \text{N}, 145^\circ 48.1' \text{E})$  from the west to east, respectively.

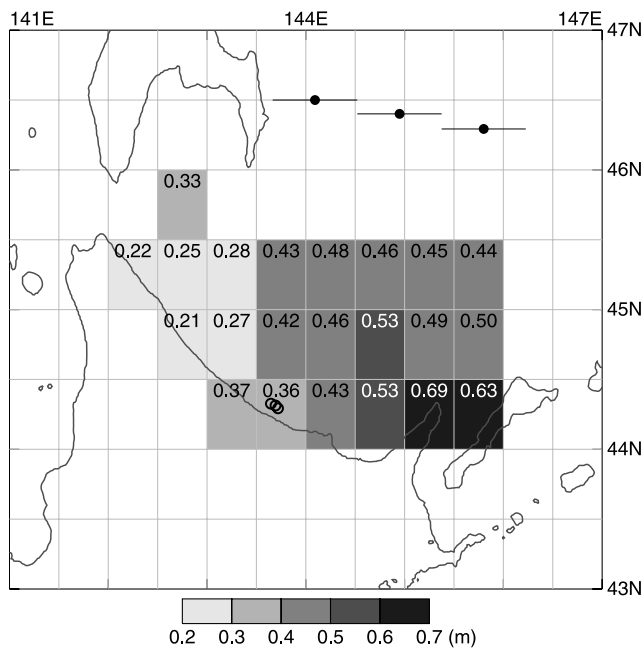


**Figure 3.** The average sea ice thicknesses in  $0.5^\circ \times 0.5^\circ$  regions in the southwestern Sea of Okhotsk during 1996–2004 based on the video-monitoring data in early February. The total number of data is 25664 over 9 years. The mooring locations are denoted by open circles. The sections centered at the SSM/I grids (solid circles) used for the ice transport estimate are also shown off the southern Sakhalin (see section 5.2).

the ocean bottom. With these instrument depths, the IPS viewed a spot of  $\sim 2$  m in diameter and the two opposite ADCP beams viewed spots  $\sim 30$  m apart at the ocean surface. The IPS sampling intervals were 1 second for range and echo amplitude data and 1 minute for pressure, tilt, and temperature data. The ADCP measured ice velocity using the bottom-tracking mode as well as water column velocity using the water-tracking mode [Melling *et al.*, 1995]. Its sampling interval was 15 min and the bin size for water column velocity was 4 m. The accuracy of the ADCP speed is less than  $0.01 \text{ m s}^{-1}$ . Atmospheric pressure data used to process the IPS data and surface wind data used to process the ADCP data were measured at stations of the Japan Meteorological Agency in Mombetsu and Yubetsu, respectively (see Figure 1 for their locations).

[9] The methods of data processing carried out in this research essentially follow previous work in the Beaufort Sea [Melling and Riedel, 1995, 1996]. General discussions on the IPS data processing are given by Melling *et al.* [1995] and Strass [1998] and detailed procedures are described by *ASL Environmental Sciences* [2003]. We calibrated sound speed

required for calculation of ice draft on the basis of range data during open water periods without large waves. Our high sampling rate of range at every second facilitated distinguishing waves and associated air bubbles from sea ice. The ice velocity data are used to convert the draft time series into the pseudo spatial series (see Figure 4). For this purpose, a continuous time series of ice velocity is necessary to estimate the width of the ice-free areas and therefore ice concentration. To estimate ice velocity within data gaps, a multilinear regression of ice velocity against near-surface water velocity from the uppermost ADCP bin centered at a depth of 5–7 m and surface wind measured in Yubetsu is performed. The draft data discussed in the following sections are the pseudo spatial series at every 0.5 m obtained by combining the draft time series and the resultant continuous ice velocity data (Figure 4). Representative values for both the accuracy and precision of draft are about  $\pm 0.05$  m.

[10] The results for the 1999 data set differ from those reported by Fukamachi *et al.* [2003], because a lower threshold of draft was used here to discriminate ice from ice-free water. This is because some thin ice portions were identified as open water in the previous data set. The reprocessed data set results in the higher concentration, and lower mean draft and deformed ice ratio since more thin ice portions are kept.

[11] The region of observation (Figure 1) is close to the southern limit of sea ice in this sea (Figure 2). The average ice velocity field derived from the SSM/I data during January–March periods of 1999–2001 shows that the ice reaching this region originates mostly from the region off the east coast of the southern half of Sakhalin (Figure 5). (The ice velocity is derived by following the displacement of brightness temperature features in sequential SSM/I imagery using the maximum cross-correlation method [Kimura and Wakatsuchi, 2000].) Thus the mooring location is suitable for observing sea ice subject to both dynamic and thermodynamic processes farther north. However, the moored data were obtained only at the nearshore locations. Therefore it is important to evaluate whether they are representative in the southwestern part of the sea. For this purpose, the distribution of the average ice thickness based on the video-monitoring data during 1996–2004 [Toyota and Wakatsuchi, 2001; Toyota *et al.*, 2004] is examined (Figure 3). Although the temporal coverage of these data used to construct this distribution is limited to early February and the method is not capable of measuring thick floes, they are the sole available data covering the entire southwestern part for nearly ten years. The ice thickness tends to increase from the west to east along the Hokkaido coast since the deformed ice from the north is absent in the western region and local deformation is likely more active in the eastern region because of the presence of land

**Table 1.** Mooring Information

Year	Location (IPS)	Mooring Period	Ice Observed Period
1999	44°19.6'N, 143°38.8'E	5 Dec 1998–27 Mar 1999	9 Feb–27 Mar (47 days)
2000	44°18.8'N, 143°41.6'E	12 Dec 1999–4 Apr 2000	23 Jan–1 Apr (70 days)
2001	44°17.6'N, 143°43.1'E	26 Nov 2000–22 Mar 2001	6 Jan–21 Mar (75 days)

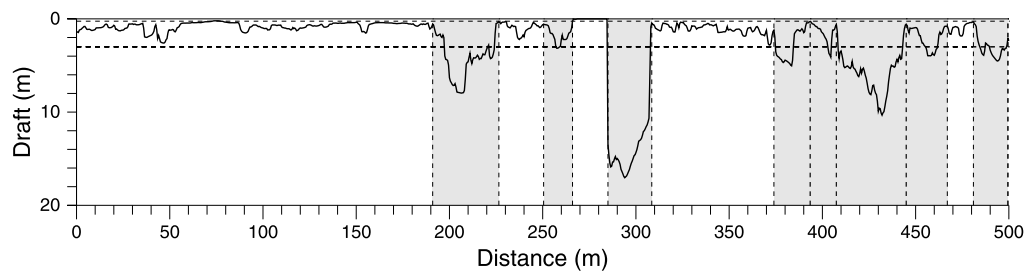


**Figure 4.** An example of draft pseudo spatial series (topographic profile) obtained by combining the IPS draft data and ADCP ice velocity data during 6 March 1999. The vertical scale is exaggerated five times with respect to the horizontal scale. Widths of keels with their maximum draft deeper than 3 m (the lower dashed line) are shaded. They are identified on the basis of the Rayleigh criterion with the reference level of 0.25 m (the upper dashed line). Vertical dashed lines are boundaries of independent keels. Note that this example contains the deepest keel found in the 3 years.

boundaries. The thickness in the region around the mooring locations (0.36 m) is between those in the western (0.21 m) and eastern (0.69 m) coastal regions and somewhat smaller than those in the offshore region (up to 0.48 m). Overall, the thickness around mooring locations is somewhat smaller than the average over the entire southwestern part (0.42 m) in the beginning of sea ice season.

## 4. Results

### 4.1. Ice Drift

[12] Cumulative ice drifts for three years during the sea ice observed period (Table 1) clearly indicate the general southeastward ice movement along the coast (Figure 6). The average vector speed was  $0.16 \text{ m s}^{-1}$  in the direction rotated  $126^\circ$  clockwise from the true north over the three years. The speed varied largely in the range from zero to  $1.16 \text{ m s}^{-1}$ . The ice velocity was well correlated with the near-surface water velocity and also affected by the local wind. These displacements indicate that the reversal of ice velocity was quite rare. Cumulative displacements were 887, 1230, 1217 km in 1999, 2000, and 2001, respectively. Note that

the short displacement in 1999 was mainly due to the short ice-observed period (Table 1).

### 4.2. Ice Draft

#### 4.2.1. Seasonal Variability

[13] Various ice statistics are calculated mostly for 40 km long subsections of the draft spatial series (Figures 7–9). The length of the subsections is chosen following *Melling and Riedel* [1995] to derive draft statistics with useful confidence. Ice concentration in some subsections, however, is too low to yield representative statistics. Unlike the similar studies in regions of high sea ice concentration, open water portions are excluded to derive draft statistics because of low concentration here. Ice concentration is defined as a ratio between numbers of nonzero draft and all the observations for each subsection (Figures 7a–9a). Ice sections in the draft spatial series are separated into sections of level and deformed ice (see Figures 7b–9b and 7c–9c). Here, a section is classified as level ice if its draft varied by less than  $\pm 0.15 \text{ m}$  over 10 m or longer. This more restrictive criterion than the  $D_2$  definition by *Wadhams and Horne* [1980], which allows variations within  $\pm 0.25 \text{ m}$ , is adopted

**Table 2.** Ice Statistics<sup>a</sup>

Period (Subsection)	Length, km	Draft, m					Level Ice	Conc., %	Deformed Ice	
		Mean	S. D.	90%	99%	Max.			Area, %	Volume, %
1999										
9–28 Feb (1–7)	275	0.37 (0.20)	0.44	0.79	2.32	7.28	0.20	54	38	67
28 Feb–6 Mar (8)	170	— (0.00)	—	—	—	—	0	—	—	—
6–27 Mar (9–19)	442	0.77 (0.26)	1.10	1.81	5.54	17.04	0.25	33	55	85
9 Feb–27 Mar (All)	887	0.60 (0.24)	0.90	1.35	4.79	17.04	0.22	40	48	81
2000										
23 Jan–2 Mar (1–13)	520	0.77 (0.61)	0.70	1.66	3.23	10.98	0.27	78	64	87
2 Mar–1 Apr (14–25)	770	0.52 (0.09)	0.64	1.18	3.07	12.09	0.18	17	44	73
23 Jan–1 Apr (All)	1230	0.72 (0.31)	0.70	1.59	3.21	12.09	0.25	43	59	85
2001										
6 Jan–2 Feb (1–8)	380	0.45 (0.18)	0.61	1.01	3.21	6.67	0.20	40	39	73
2–2 Feb (9)	140	— (0.00)	—	—	—	—	0	—	—	—
7–28 Feb (10–18)	360	0.39 (0.32)	0.48	0.95	2.33	10.03	0.20	81	32	66
28 Feb–21 Mar (19–26)	337	0.70 (0.34)	0.83	1.67	4.07	10.54	0.27	48	50	81
14 Jan–21 Mar (All)	1217	0.49 (0.25)	0.64	1.17	3.20	10.54	0.21	50	39	73
1999–2001										
All	3334	0.60 (0.27)	0.73	1.40	3.56	17.04	0.23	45	48	80

<sup>a</sup>For the draft statistics, areas of zero draft are excluded except for the mean drafts in parentheses. S.D. is the abbreviation for standard deviation. Values for 90 and 99% indicate drafts that exceed these percentiles among the all the drafts sorted in increasing order.

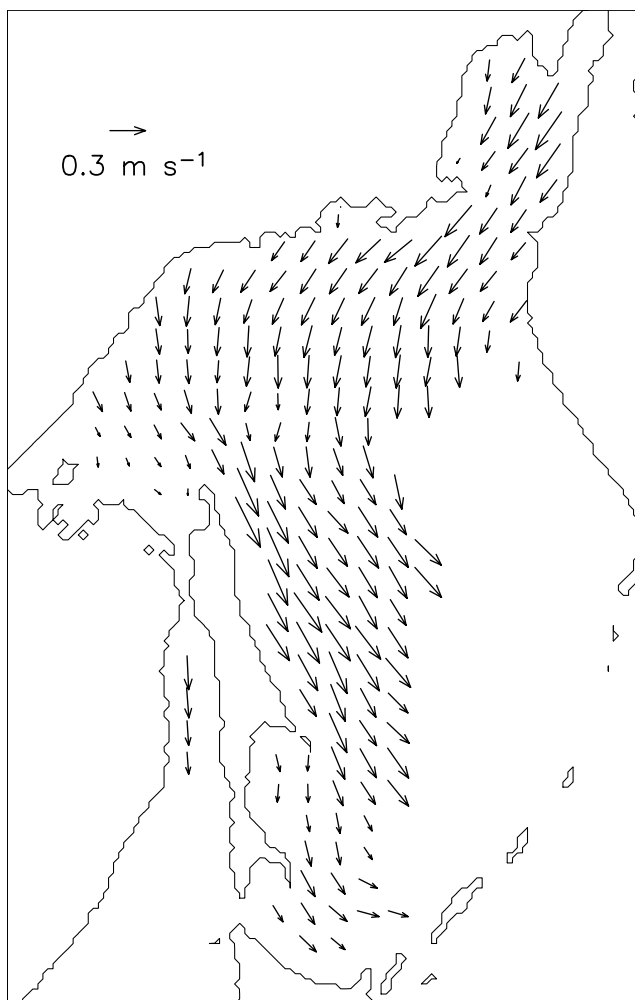


**Figure 5.** The averaged ice velocity field during January–March periods in 1999–2001 derived from the SSM/I data. Vectors are drawn only for the grids with more than 80 daily velocity estimates over the three winters combined.

because drafts for level ice were thinner than those in other data obtained in polar regions. Ridge keels (see Figures 7d–9d and 7e–9e) are identified using the Rayleigh criterion [Wadhams and Davy, 1986] with a reference level of 0.25 m (Figure 4). This reference level is chosen close to the mean draft of level ice for the three years (0.23 m listed in Table 2). The first five ice categories in Figures 7f–9f roughly correspond to those of nilas, young ice, thin, medium, and thick first-year ice, which are defined in terms of thickness.

[14] In 1999, there was a marked contrast in February and March. Generally, February was characterized by the lower mean drafts of all and deformed ice (Figure 7b) and deformed ice ratios (Figure 7c) and less and shallower keels (Figures 7d and 7e) and less thicker ice (Figure 7f), and March was characterized by the opposite features. Their monthly statistics are summarized in Table 2. The transition between these two states occurred from the end of February to beginning of March when two intense atmospheric low-pressure systems passed the region of observation. This transition indicates the advection of deformed ice likely caused by strong winds. Note that the deepest keel of

~17 m over the three years was observed in the beginning of March shortly after this transition (Figure 7e).

[15] In 2000, the seasonal variability was almost opposite from that in 1999. Generally, February including late January was characterized by the higher mean drafts of all and deformed ice (Figure 8b) and deformed ice ratios (Figure 8c) and more thicker ice (Figure 8f), and March was characterized by the opposite features. On the other hand, there are no marked differences in keel statistics in these two months except the frequency was quite high in mid-February (Figures 8d and 8e).

[16] In 2001, the seasonal variability was somewhat similar to that in 1999. Generally, January and February were characterized by the lower mean drafts of all and deformed ice (Figure 9b) and deformed ice ratios (Figure 9c) and less thicker ice (Figure 9f), and March was characterized by the opposite features. The keel frequency was higher in January as well as in March (Figure 9d). Note that the above characteristics in January and February were especially distinct in mid-February following the no-ice period (Figures 9b, 9c, and 9f).

[17] Unlike the other ice statistics described above, the mean draft of level ice did not change appreciably during all the months in the three years (Figures 7b–9b). (Note that relatively large values exceeding 0.5 m occurred only when the deformed ice ratios were quite high.) Its range (0.18–0.27 m) was smaller than that of all ice (0.37–0.77 m) (Table 2). This suggests that the thermodynamic growth is not likely responsible for the overall draft increase.

#### 4.2.2. Yearly and 3-Year Averages

[18] Ice statistics summarized in Table 2 clearly show the yearly differences. The mean draft (0.72 m) and deformed-

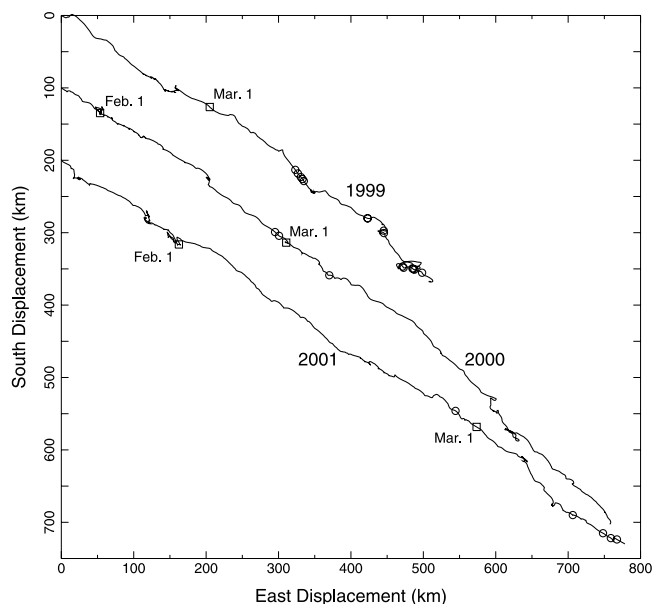


**Figure 6.** Cumulative ice drifts for three winters based on sea ice velocity measured by an ADCP. For clarity the drifts in 2000 and 2001 are offset southward by 100 and 200 km, respectively. Positions on 1 February and 1 March are denoted by squares. Positions of keels deeper than 9 m are denoted by circles. Note that some of the circles are completely overlapped. (See discussions in section 4.2.2).

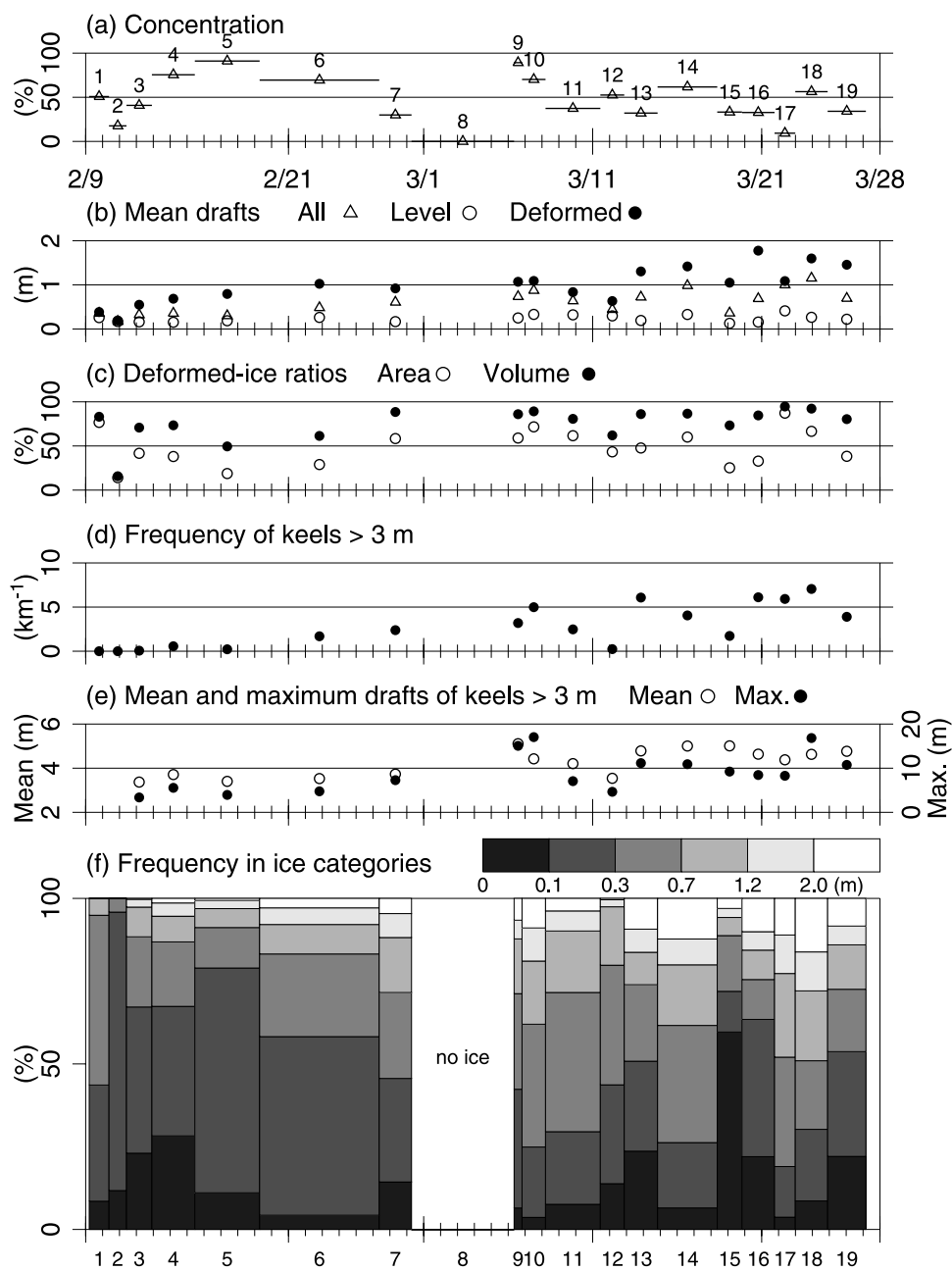


**Figure 7.** Time series of (a) ice concentration, (b) mean drafts, (c) deformed ice ratios, (d) frequency of keels deeper than 3 m defined over ice sections, (e) mean and maximum drafts of keel deeper than 3 m, and (f) frequency in ice categories in 1999. Values are plotted for subsections with a length of 40 km except subsections 7, 8, and 19 of 35, 170, and 42 km long, respectively. Periods of subsections are denoted by horizontal bars in Figure 7a and their numbers are displayed in Figures 7a and 7f. In Figure 7b, the mean drafts for all, level, and deformed ice are plotted. In Figure 7c, the deformed ice ratios for area and volume are plotted. In Figure 7f, ice categories are defined as shown in the gray scale.

ice ratios (areal 59 and volumetric 85%) were the highest in 2000. On the contrary, the mean draft (0.49 m) and deformed ice ratios (areal 39 and volumetric 73%) were the lowest in 2001. These values were in between in 1999. Note that the deformed ice dominated ice volume even in 2001 when the deformed ice ratios were the lowest. In the three years, the overall mean draft, and areal and volumetric deformed ice ratios were 0.60 m, and 48 and 80%, respec-

tively. The dominance of deformed ice indicates that the dynamic processes such as rafting and ridging play important roles in the draft evolution. The similar dominance of deformed ice was previously discussed by *Melling and Riedel* [1995, 1996] in the Beaufort Sea and by *Worby et al.* [1996] in the Bellingshausen and Amundsen seas.

[19] Drafts of 90 and 99 percentiles along with the maximum value in Table 2 represent the thicker end of

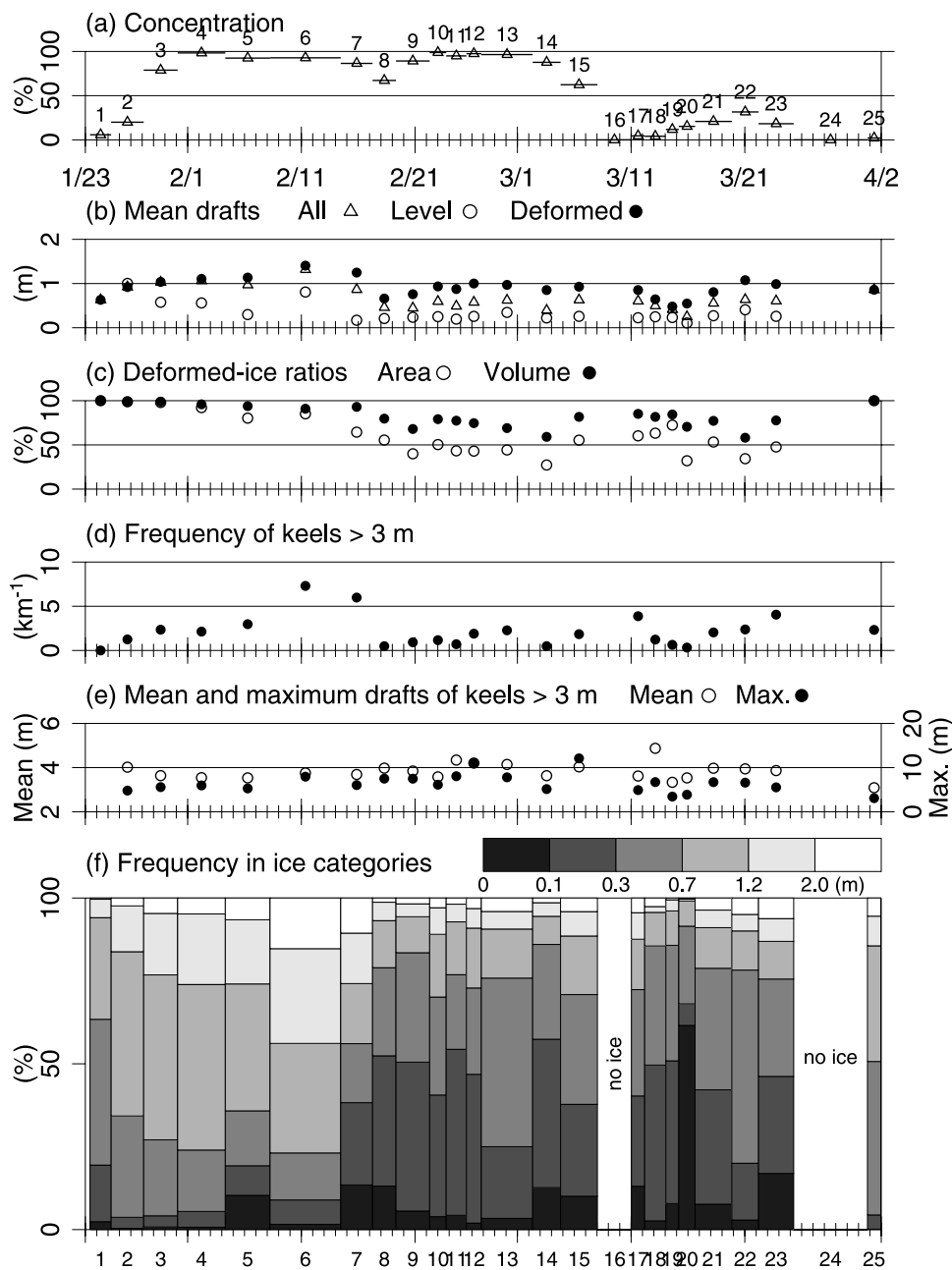


**Figure 8.** Similar to Figure 7 except in 2000. Subsections 15, 16, 23, 24, and 25 are 60, 110, 50, 190, and 20 km in length, respectively.

ice distribution. The 99-percentile draft was by far the largest in 1999 (4.79 m). The 90-percentile draft was the lowest in 2001 (1.17 m). In order to reveal ice draft distribution in each year and the three years combined in more detail, its probability density in the draft range of 0–10 m is examined (Figure 10). As indicated in Table 2, the probability density for drafts >3 m was appreciably higher in 1999 (red circles) than in 2000 (green circles) and 2001 (blue circles). Also, the density for drafts in 1–3 m was higher in 2000 than in 1999 and 2001. For draft  $d$  in the range of 3.4–10 m, the probability density  $f(d)$  can be represented by the exponential function  $f(d) = a \exp(-d/b)$ , where  $a$  and  $b$  are 0.214 and 1.37, 0.137 and 1.08, 0.094

and 1.18, and 0.129 m<sup>-1</sup> and 1.26 m in 1999, 2000, 2001, and 1999–2001, respectively. (These functions are plotted as straight lines in the figure.) The overall  $e$ -folding scale  $b$  is much smaller than those evaluated in polar regions. The  $e$ -folding scales evaluated in Beaufort Sea are 2–4 m for the roughly same draft range [Melling and Riedel, 1995, 1996] and ~3 m in Fram Strait even for the range of 10–25 m [Vinje *et al.*, 1998]. The value obtained here is closer to ~1.5 m for drafts >4 m evaluated using submarine sonar data in the southern part (61–65°N) of Davis Strait west of Greenland [Wadhams *et al.*, 1985]. Thus the ratio of thick ice is lower in the Sea of Okhotsk than those in polar regions and closer to that in relatively low latitudes. In the

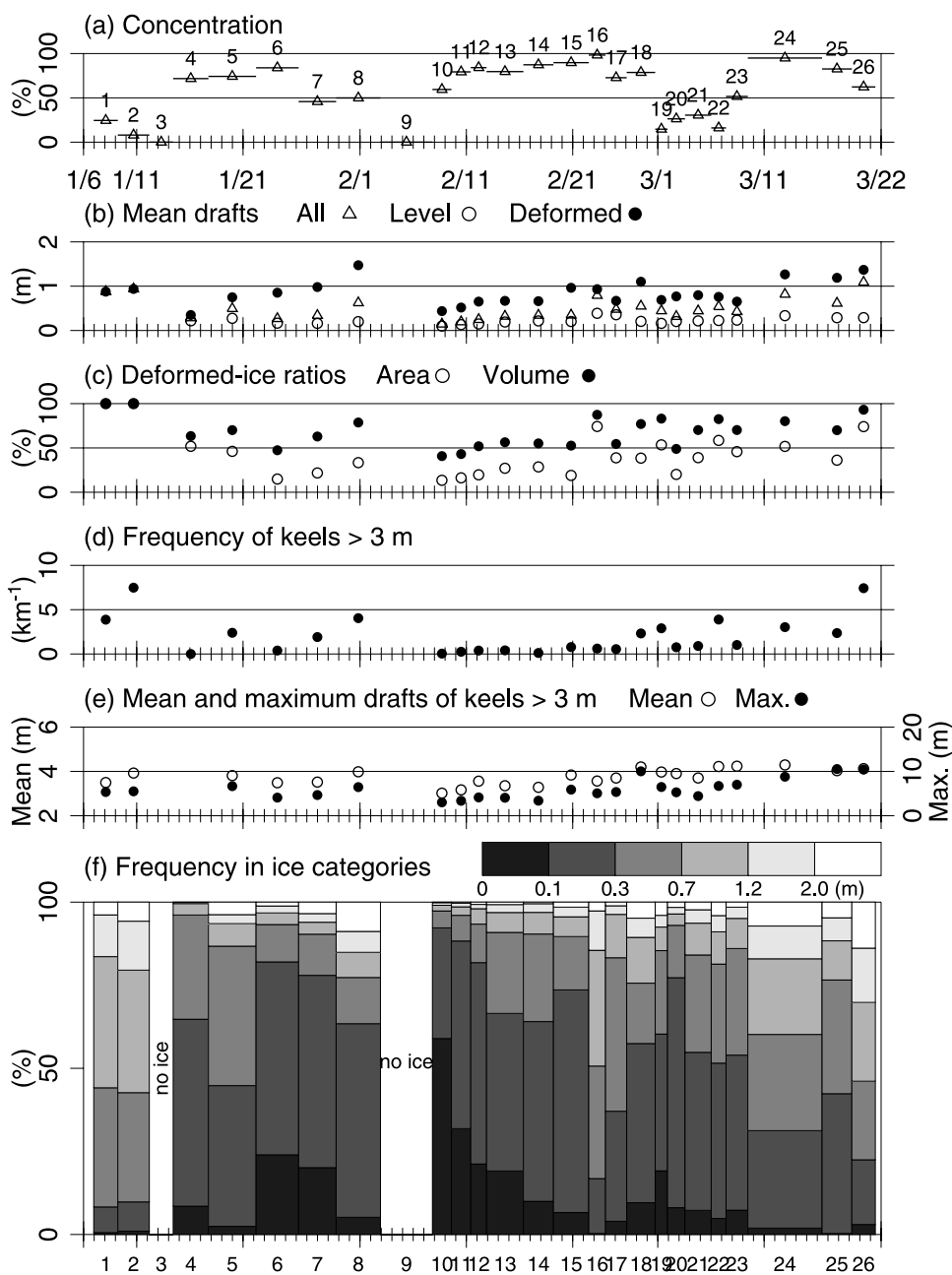


**Figure 9.** Similar to Figure 7 except in 2001. Subsections 3, 8, 9, and 26 are 75, 65, 140, and 57 km in length, respectively.

draft range of about 1–3 m, different exponential curves with larger  $e$ -folding scales can be fit. The fact that two curves can be fit to each probability density might be indicative of a mixing of ice with different origins or different growth history. *Wadhams et al.* [1985] obtained the similar probability density in Davis Strait. Note that the probability density for level ice (triangles in Figure 10) is quite low for draft exceeding 1 m.

[20] Keel statistics summarized in Table 3 clearly show that more deeper keels with the maximum draft >5 m were observed in 1999 than in 2000 and 2001. Even the keel frequencies in 1999, however, are one or two orders lower than those observed in the polar regions such as the Arctic Canadian Basin [*Wadhams and Horne*, 1980] and Beaufort

Sea [*Melling and Riedel*, 1995, 1996] where the mean drafts are 2–4 m. The frequencies in Table 3 are comparable only to those observed in Davis Strait where the mean draft is ~1 m [*Wadhams et al.*, 1985].

[21] Following *Wadhams* [1983], *Wadhams et al.* [1985], and *Melling and Riedel* [1995, 1996], the distribution of keel frequency is examined whether the extreme drafts are observed more often than those predicted by the extrapolation of observed keel frequencies at common keel drafts (3.5–10.5 m) to rare keel drafts (Figure 11). The exponential function fitted (the line in the figure) has an  $e$ -folding scale of 1.25 m. The extrapolation of the exponential function shows that the observed keels with drafts >15 m (three of them) were anomalously deep.

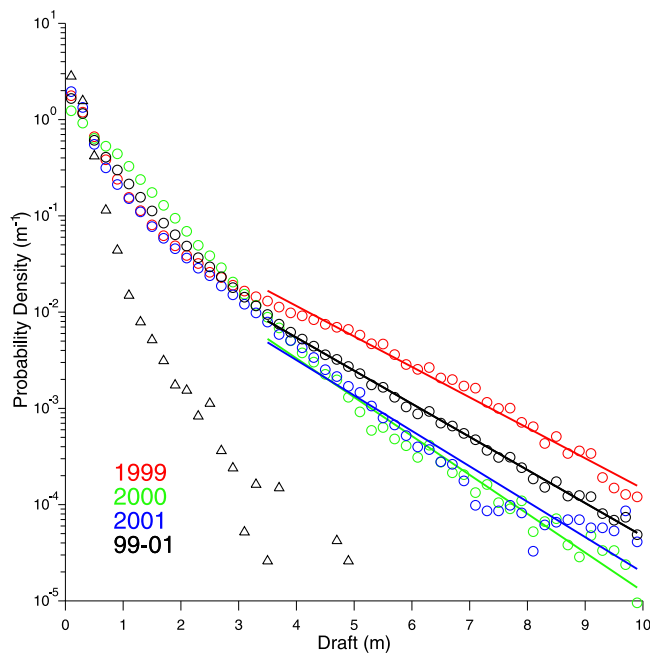


**Figure 10.** Probability density of the draft for 1999, 2000, and 2001 (red, green, and blue circles) and three years combined (black circles). The bin size is 0.2 m. Their exponential functions between 3.4 and 10 m draft are also plotted. Probability density of the level ice draft is also shown (triangles).

[22] As in the Arctic discussed by *Wadhams* [1978], deep keels were heavily clustered together in several occasions as shown in Figure 6. For keels deeper than 9 m, only 4 keels were isolated without any similar deep keels within 10 km. Other 24 deep keels occurred in 8 clusters in the three years. This suggests that each cluster of deep keels was formed in a single intense deformation event such as a strong low pressure and these keels stayed close together as discussed

by *Wadhams* [1978]. The small number of such deep keels suggests that such an intense deformation event is not frequent in the Sea of Okhotsk.

## 5. Discussion

### 5.1. Control Factors of Draft

[23] It was shown that the mean draft is strongly controlled by the deformed ice ratio in section 4.2 (Figures 7b–9b and 7c–9c and Table 2). Here, this relationship is more closely examined (Figure 12). A linear regression of the mean draft against the areal deformed ice ratio is performed using the data from subsections which contained both the level and deformed ice. The linear regression line for the mean draft  $d$  is  $d = 0.112 + 0.958 \cdot DR$ , where  $DR$  is the areal deformed ice ratio. A high correlation coefficient of 0.784 indicates that the mean draft can be estimated fairly well by the deformed ice ratio. Note that this relationship was clearly seen for all three winters. Although the statistics in each subsection are not completely independent, it is safe to say that there are at least three phases of quite different draft characteristics in the time series every year (Figures 7b–9b and 7c–9c). Thus this correlation coefficient is significantly different from zero at the 95% confidence level at least. Using the data from the same subsections, the linear regression analyses of the mean draft against the level ice draft, and the level ice draft against the deformed ice ratio are also performed. Correlation coefficients are 0.663 and 0.682 for these two relationships. These coefficients suggest that the level ice draft is also related to the mean draft and the deformed ice ratio is also related to the level ice draft. However, a multilinear regression of the mean draft against the level ice draft and deformed ice ratio yields a correlation coefficient of 0.803, which is not much better than 0.784 for the linear regression against the deformed ice ratio alone. In conclusion, the mean draft can be estimated fairly well by the deformed ice ratio alone in the region of observation. The similar relationship between the mean draft and deformed ice (level ice) ratio

**Table 3.** Keel Statistics<sup>a</sup>

	9 m	7 m	5 m	3 m
<i>1999</i>				
Number of keels	20	82	277	912
Keels per kilometer	0.06 (0.02)	0.23 (0.09)	0.79 (0.31)	2.59 (1.03)
Mean of maximum keel drafts, m	10.86	8.44	6.55	4.59
<i>2000</i>				
Number of keels	3	17	89	1222
Keels per kilometer	0.006 (0.002)	0.03 (0.01)	0.17 (0.07)	2.33 (0.99)
Mean of maximum keel drafts, m	10.79	8.20	6.13	3.80
<i>2001</i>				
Number of keels	5	16	139	1029
Keels per kilometer	0.008 (0.004)	0.03 (0.01)	0.23 (0.11)	1.69 (0.85)
Mean of maximum keel drafts, m	10.19	8.51	6.00	3.99
<i>1999–2001</i>				
Number of keels	28	115	505	3163
Keels per kilometer	0.02 (0.008)	0.08 (0.03)	0.34 (0.15)	2.13 (0.95)
Mean of maximum keel drafts, m	10.74	8.41	6.32	4.09

<sup>a</sup>Values are listed for keels deeper than 9, 7, 5, and 3 m. For the keel frequency both of the values over ice portions only and all the portions including open water (in parentheses) are shown.

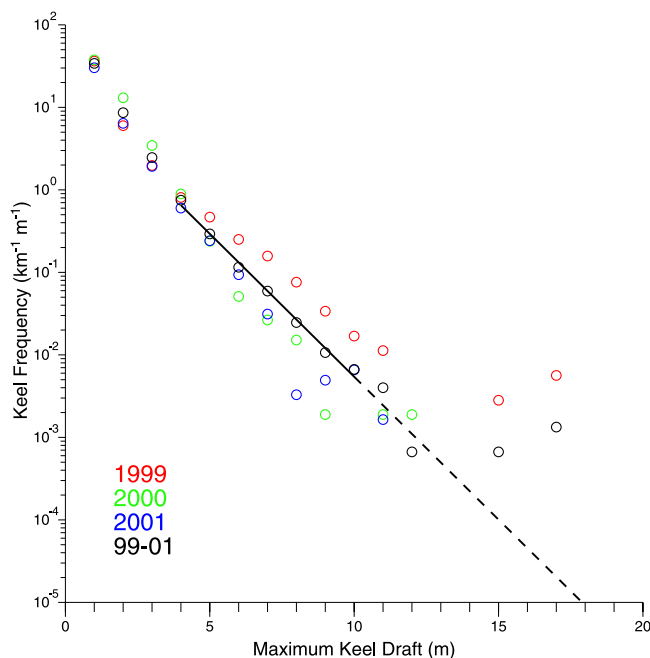


**Figure 11.** Frequency of keels for 1999, 2000, and 2001 (red, green, and blue circles) and 1999–2001 (black circles). The bin size is 1 m. The exponential function for 1999–2001 between 3.5 and 10.5 m draft is also plotted.

has been discussed in the Arctic [Wadhams, 1981] and Davis Strait [Wadhams *et al.*, 1985].

[24] By ship-based visual observation, it is impossible to evaluate the mean draft including deep keels. On the other hand, it is possible to evaluate the areal deformed ice ratio to some extent. Since the ship-based visual observations following the Antarctic Sea Ice Processes and Climate (ASPeCt) program guidelines [Worby, 1999] have been carried out in this region since 1997 [Toyota, 1998], we can possibly estimate the mean draft from the observed deformed ice ratio in this visual observation data set.

## 5.2. Ice Transport Estimate to the Southwestern Sea of Okhotsk

[25] In this section, we attempt to estimate ice transport into the southwestern Sea of Okhotsk in order to understand the heat and freshwater budgets. Because of the lack of sea ice thickness data, however, it has been impossible to carry out such an estimate without assuming the thickness. Ohshima *et al.* [2003] roughly estimated the southward ice transport as  $\sim 120 \text{ km}^3$  (corrected from the figure of  $\sim 230 \text{ km}^3$  misprinted in their paper) assuming the southward drift speed of  $0.3 \text{ m s}^{-1}$ , the width of southward flowing region of 100 km, and the ice transport period of 3 months along with the average ice thickness of 0.5 m.

[26] Here, the southward ice transport is estimated using the measured ice thickness for the first time (Figure 13). The transport is calculated at a  $\sim 200 \text{ km}$  section off the east coast of the southern Sakhalin using monthly mean values of concentration and meridional speed evaluated at three SSM/I grids shown in Figures 2 and 3. This is because thermodynamic growth is limited below 1 cm per day even in the middle of winter in the region off Hokkaido [Toyota

*et al.*, 2000] and the examination of the ice concentration (Figure 2) and velocity fields (Figure 5) derived from the SSM/I data suggests that this section captures most of the southward ice transport into this region. According to the video-monitoring data, the ice thickness observed in the vicinity of the mooring locations was close to the mean thickness over the region off Hokkaido (see Figure 3). Thus the draft observed by the IPS moorings is used for this estimate. Assuming isostasy, the measured draft is converted to thickness using densities of near-surface water of  $1026 \text{ kg m}^{-3}$  based on the CTD observations [Ohshima *et al.*, 2001] and sea ice of  $864 \text{ kg m}^{-3}$  based on sample core measurement [Toyota, 1998] in the region off Hokkaido. Namely, the overall mean draft of 0.60 m results in a thickness of 0.71 m.

[27] The concentration was negligible in December and the largest in March (Figure 13a). The southward speed was the largest in January or February and the northward speed was also seen in April (Figure 13b). Cumulative ice transport values estimated using the yearly mean thickness converted from the corresponding drafts (Table 2) are  $\sim 15$ , 70, and  $56 \text{ km}^3$ , in 1999, 2000 and 2001, respectively (Figure 13c). These values are  $\sim 15$ , 58, and  $65 \text{ km}^3$  if the overall mean thickness over all three years of 0.71 m is used. In 2000 and 2001, the use of the yearly mean thickness changes the resultant transport significantly from that derived with the overall mean thickness. The ice transport in 1999 was much smaller than in other two years. Since the concentration in 1999 was comparable to those in other years, this was mainly due to the slower southward speed then. Note that the ice transport based on the yearly mean thickness is larger in 2000 than in 2001 despite the

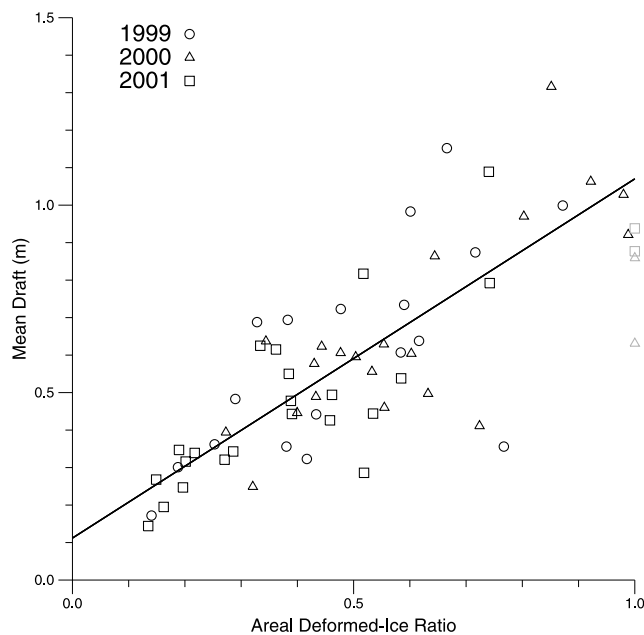


**Figure 12.** A scatter diagram between the areal deformed ice ratio and mean draft in each subsection. Data in 1999, 2000, and 2001 are shown by circles, triangles, and squares, respectively. Those plotted in gray are the data in subsections without level ice. A regression line is obtained using only the data plotted with black symbols.

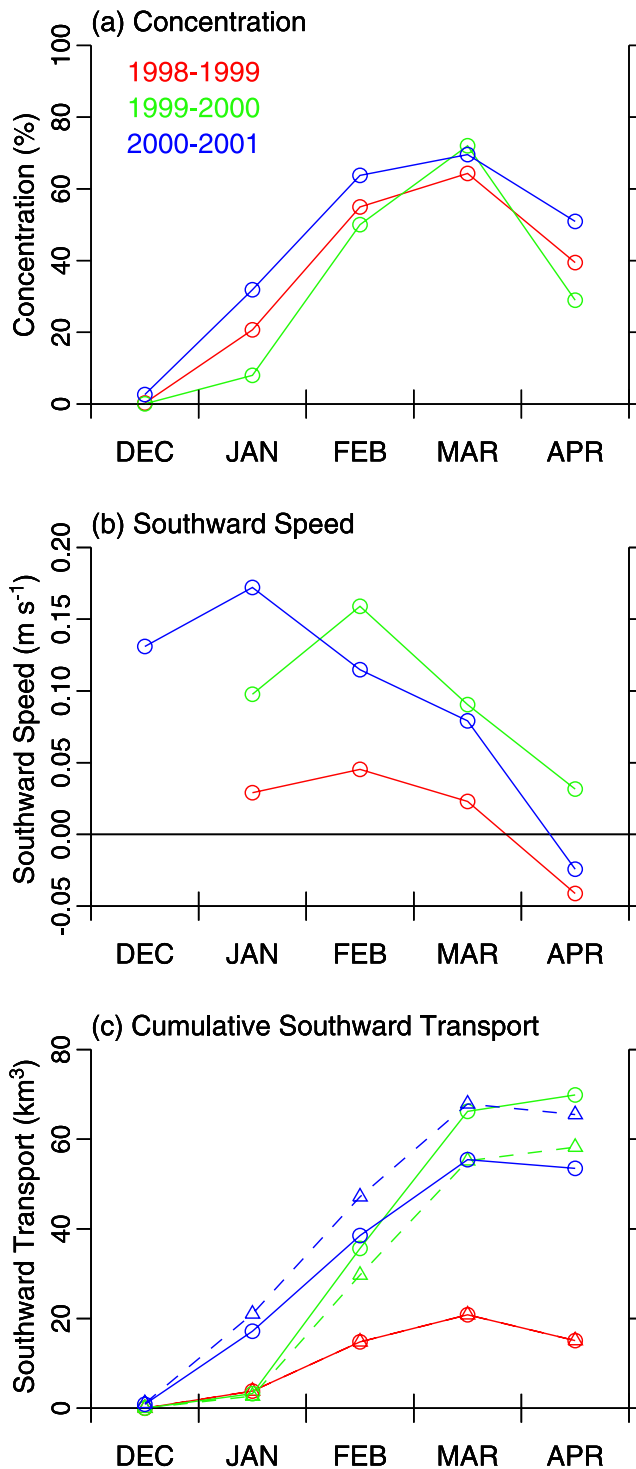


**Figure 13.** (a) Monthly mean sea ice concentration and (b) southward speed averaged over the three SSM/I grids off the southern Sakhalin shown in Figures 2 and 3. Values for 1998–1999, 1999–2000, and 2000–2001 are shown by red, green, and blue symbols, respectively. (c) Cumulative ice transport estimated on the basis of the yearly and overall mean thicknesses are denoted by circles and triangles, respectively.

smaller maximum ice extent in the entire sea and the lower concentration in the southwestern part. These results suggest that the magnitude of the southward speed is the most important factor determining the yearly variability of ice transport but the ice thickness is also a significant factor. In turn, the magnitude and direction of wind govern the ice transport since the magnitude of the southward flowing East Sakhalin Current does not change considerably from year to year [Mizuta *et al.*, 2003]. The primary importance of atmospheric forcing and the secondary importance of ice thickness on the interannual variability of ice transport were also found in Fram Strait by Vinje *et al.* [1998]. Except in 1999, the estimated transport is somewhat smaller than the rather rough estimate by Ohshima *et al.* [2003].

[28] Associated heat and freshwater transport is derived from the estimated ice transport. Using the ice density of  $864 \text{ kg m}^{-3}$  and latent heat of fusion of  $302 \text{ kJ kg}^{-1}$ , heat transport values are  $-3.9 \times 10^{17}$ ,  $-1.8 \times 10^{18}$ , and  $-1.5 \times 10^{18} \text{ J}$  in 1999, 2000, and 2001, respectively. For the freshwater transport estimate, the salinities of the near-surface water of 32.5 based on the climatological data set [Itoh and Ohshima, 2000] and sea ice of 6 based on sample core measurement [Toyota, 1998] in the region off Hokkaido are assumed. The resultant freshwater transport is  $\sim 12$ , 57, and  $46 \text{ km}^3$  in 1999, 2000, and 2001, respectively. These values correspond to  $\sim 4$ , 20, and 16% of the annual Amur River discharge (see the inset map in Figure 1 for its location) of  $291 \text{ km}^3$  (data provided by the Global Run-off Data Center, Germany), which is a major freshwater source for the Sea of Okhotsk. Considering the fact that only the part of the Amur River discharge is transported to the southwestern part, the freshwater transport by sea ice is not negligible there.

## 6. Summary

[29] In this research, the average draft and keel statistics in the Sea of Okhotsk were derived by the moored sonar observations for the first time. The mean draft of 0.60 m (0.71 m in thickness), thick ice ratio, and keel frequency are smaller than those in the similar data obtained in the polar regions. For example, the mean draft is 3.15 m in Beaufort Sea [Melling and Riedel, 1995] and the mean thickness is 3.27 m in Fram Strait [Vinje *et al.*, 1998]. These characteristics are closer to the submarine sonar data obtained in Davis Strait located at lower latitudes [Wadhams *et al.*, 1985]. It is shown that the variability of the mean draft is related to that of the deformed ice ratio fairly well. The southward ice transport, which accompanies heat and freshwater transport, is also estimated using the observed ice thickness for the first time.

[30] The major limitation of this research is that the mooring observations were carried out only in the region very close to Hokkaido, where the microwave remote sensing data are not usable because of the land contamination. Obviously, the accumulation of more moored data in other regions of the Sea of Okhotsk is crucial to enhance our understanding of the nature of ice thickness and volume. In addition, moored data in the region away from the land mass will enable comparisons with ice type [Kimura and Wakatsuchi, 1999] and thickness data [Tateyama and Enomoto, 2001] which have been derived from the micro-

wave remote sensing data. Thus they will be valuable sea truth data for developing the algorithm to estimate sea ice thickness using the microwave data. Furthermore, combining the sea ice velocity data derived from the sea ice radar data in the region near Hokkaido [e.g., *Tabata et al.*, 1980] and/or the high-resolution microwave data obtained by the AMSR-E and AMSR sensors with the moored data should enable us to identify the location of deformation for the deformed ice observed at the mooring sites. We are currently planning to investigate these, and other related, issues.

[31] **Acknowledgments.** We are deeply indebted to Humfrey Melling, David Fissel, and Bob Lane for their advice for the observations. We also thank Dave Billenness for his assistance in data processing. Logistical support was provided by Yubetsu Fishermen's Union, Sanyo-Techno Marine, and Sea Ice Research Laboratory of Hokkaido University. This work was supported by funds from the Core Research for Evolutional Science and Technology of the Japan Science and Technology Corporation, from the Research Revolution 2002 (RR2002) of Project for Sustainable Coexistence of Humans, Nature and the Earth, and from Grant-in-Aid 12740266 and 17540405 for scientific research from Ministry of Education, Science, Sports, and Culture of Japan. Figures were produced by the PSPLOT and GFD DENNOU Libraries.

## References

- ASL Environmental Sciences (2003), *ASL IPS Processing Toolbox User's Guide*, 111 pp., ASL Environ. Sci. Inc., Sidney, B. C., Canada.
- Birch, R., D. Fissel, H. Melling, K. Vaudrey, K. Schaudt, J. Heideman, and W. Lamb (2000), Ice-profiling sonar, *Sea Technol.*, *41*, 48–52.
- Drucker, R., S. Martin, and R. Moritz (2003), Observations of ice thickness and frazil ice in the St. Lawrence Island polynya from satellite imagery, upward looking sonar, and salinity/temperature moorings, *J. Geophys. Res.*, *108*(C9), 3149, doi:10.1029/2001JC001213.
- Fukamachi, Y., G. Mizuta, K. I. Ohshima, H. Melling, D. Fissel, and M. Wakatsuchi (2003), Variability of sea-ice draft off Hokkaido in the Sea of Okhotsk revealed by a moored ice-profiling sonar in winter of 1999, *Geophys. Res. Lett.*, *30*(7), 1376, doi:10.1029/2002GL016197.
- Harms, S., E. Fahrbach, and V. Strass (2001), Sea ice transports in the Weddell Sea, *J. Geophys. Res.*, *106*, 9073–9557.
- Ishikawa, M., T. Takatsuka, T. Daibo, K. Shirasawa, and M. Aota (2001), Distributions of pack ice in the Okhotsk Sea off Hokkaido observed using a sea-ice radar network, January–April, 2001, *Low Temp. Sci., Ser. A*, *60*, 13–40.
- Itoh, M., and K. I. Ohshima (2000), Seasonal variations of water masses and sea level in the southwestern part of the Okhotsk Sea, *J. Oceanogr.*, *56*, 643–654.
- Japan Meteorological Agency (2001), The results of sea ice observations [CD-ROM], Tokyo, Japan.
- Kimura, N., and M. Wakatsuchi (1999), Processes controlling the advance and retreat of sea ice in the Sea of Okhotsk, *J. Geophys. Res.*, *104*, 11,137–11,150.
- Kimura, N., and M. Wakatsuchi (2000), Relationship between sea-ice motion and geostrophic wind in the Northern Hemisphere, *Geophys. Res. Lett.*, *27*, 3735–3738.
- Marko, J. (2003), Observations and analyses of an intense waves-in-ice event in the Sea of Okhotsk, *J. Geophys. Res.*, *108*(C9), 3296, doi:10.1029/2001JC001214.
- Melling, H., and D. A. Riedel (1995), The underside topography of sea ice over the continental shelf of the Beaufort Sea in the winter of 1990, *J. Geophys. Res.*, *100*, 13,641–13,653.
- Melling, H., and D. A. Riedel (1996), Development of seasonal pack ice in the Beaufort Sea during the winter of 1991–1992: A view from below, *J. Geophys. Res.*, *101*, 11,975–11,991.
- Melling, H., P. H. Johnston, and D. A. Riedel (1995), Measurements of the underside topography of sea ice by moored subsea sonar, *J. Atmos. Oceanic Technol.*, *13*, 589–602.
- Mizuta, G., Y. Fukamachi, K. I. Ohshima, and M. Wakatsuchi (2003), Structure and seasonal variability of the East Sakhalin Current, *J. Phys. Oceanogr.*, *33*, 2430–2445.
- Ohshima, K. I., G. Mizuta, M. Itoh, Y. Fukamachi, T. Watanabe, Y. Nabae, K. Suehiro, and M. Wakatsuchi (2001), Winter oceanographic conditions in the southwestern part of the Okhotsk Sea and their relation to sea ice, *J. Oceanogr.*, *57*, 451–460.
- Ohshima, K. I., T. Watanabe, and S. Nihashi (2003), Surface heat budget of the Sea of Okhotsk during 1987–2001 and the role of sea ice on it, *J. Meteorol. Soc. Jpn.*, *81*, 653–677.
- Parkinson, C. L. (1990), The impact of the Siberian high and Aleutian low on the sea-ice cover of the Sea of Okhotsk, *Ann. Glaciol.*, *14*, 226–229.
- Strass, V. H. (1998), Measuring sea ice draft and coverage with moored upward looking sonars, *Deep Sea Res., Part I*, *45*, 795–818.
- Strass, V. H., and E. Fahrbach (1998), Temporal and regional variation of sea ice draft and coverage in the Weddell Sea obtained from Upward Looking Sonars, in *Antarctic Sea Ice: Physical Processes, Interactions and Variability*, *Antarct. Res. Ser.*, vol. 74, edited by M. O. Jeffries, pp. 123–139, AGU, Washington, D. C.
- Tabata, T., T. Kawamura, and M. Aota (1980), Divergence and rotation of an ice field off Okhotsk Sea coast off Hokkaido, in *Sea Ice Processes and Models*, edited by R. S. Pritchard, pp. 273–282, Univ. of Wash. Press, Seattle.
- Tateyama, K., and H. Enomoto (2001), Observation of sea-ice thickness fluctuation in the seasonal ice-covered area during 1992–99 winters, *Ann. Glaciol.*, *33*, 449–456.
- Toyota, T. (1998), A study of growth processes of sea ice in the southern region of the Okhotsk Sea, evaluated from heat budget and sea ice sample analysis, Ph.D. thesis, 143 pp., Hokkaido University, Sapporo, Japan.
- Toyota, T., and M. Wakatsuchi (2001), Characteristics of the surface heat budget during the ice-growth season in the southern Sea of Okhotsk, *Ann. Glaciol.*, *33*, 230–236.
- Toyota, T., T. Kawamura, and M. Wakatsuchi (2000), Heat budget in the ice cover of the southern Okhotsk Sea derived from in-situ observations, *J. Meteorol. Soc. Jpn.*, *78*, 585–596.
- Toyota, T., T. Kawamura, K. I. Ohshima, H. Shimoda, and M. Wakatsuchi (2004), Thickness distribution, texture and stratigraphy, and a simple probabilistic model for dynamical thickening of sea ice in the southern Sea of Okhotsk, *J. Geophys. Res.*, *109*, C06001, doi:10.1029/2003JC002090.
- Vinje, T., N. Nordlund, and Å. Kvambekk (1998), Monitoring ice thickness in Fram Strait, *J. Geophys. Res.*, *103*, 10,437–10,449.
- Wadhams, P. (1978), Characteristics of deep pressure ridges in the Arctic Ocean, in *Proceedings of the 4th International Conference on Port and Ocean Engineering Under Arctic Conditions*, vol. 1, edited by D. B. Muggerridge, pp. 544–555, Memorial Univ. of Newfoundland, St. John's, Newfoundland, Canada.
- Wadhams, P. (1981), Sea-ice topography of the Arctic Ocean in the region 70°W to 25°E, *Philos. Trans. R. Soc. London, Ser. A*, *302*, 45–85.
- Wadhams, P. (1983), The prediction of extreme keel depths from sea ice profiles, *Cold Reg. Sci. Technol.*, *6*, 256–266.
- Wadhams, P., and T. Davy (1986), On the spacing and draft distributions for pressure ridge keels, *J. Geophys. Res.*, *91*, 10,697–10,708.
- Wadhams, P., and R. J. Horne (1980), An analysis of ice profiles obtained by submarine sonar in the Beaufort Sea, *J. Glaciol.*, *25*, 401–424.
- Wadhams, P., A. S. McLaren, and R. Weintraub (1985), Ice thickness distribution in Davis Strait in February from submarine sonar profiles, *J. Geophys. Res.*, *90*, 1069–1077.
- Worby, A. P. (1999), *Observing Antarctic Sea Ice: A Practical Guide for Conducting Sea Ice Observations From Vessels Operating in the Antarctic Pack Ice* [CD-ROM], Antarct. Sea Ice Processes and Clim. Program, Comm. for Antarct. Res. Global Change, Hobart, Tasmania, Australia.
- Worby, A. P., M. O. Jeffries, W. F. Weeks, K. Morris, and R. Jaña (1996), The thickness distribution of sea ice and snow cover during late winter in the Bellingshausen and Amundsen seas, Antarctica, *J. Geophys. Res.*, *101*, 28,441–28,455.
- Worby, A. P., G. M. Bush, and I. Allison (2001), Seasonal development of the sea-ice thickness distribution in East Antarctica: Measurements from upward-looking sonar, *Ann. Glaciol.*, *33*, 177–180.

Y. Fukamachi, N. Kimura, K. I. Ohshima, T. Toyota, and M. Wakatsuchi, Institute of Low Temperature Science, Hokkaido University, Sapporo 060-0819, Japan. (yasuf@lowtem.hokudai.ac.jp)

G. Mizuta, Graduate School of Environmental Earth Science, Hokkaido University, Sapporo 060-0012, Japan. (mizuta@ees.hokudai.ac.jp)